Difference equations *versus* differential equations, a possible equivalence for the Rössler system ?

Christophe Letellier [a,*]

[a] *Université de Rouen - CORIA UMR 6614, Av. de l'Université, BP 12, F-76801 Saint-Etienne du Rouvray cedex, France*

Saber Elaydi [b]

[b] *Trinity University, Department of Mathematics, 715 Stadium Drive, San Antonio, TX 78212-7200, USA*

Luis A. Aguirre [c]

[c] *Universidade Federal de Minas Gerais, Av. Antonio Carlos 6627, Belo Horizonte 31270-901, Brazil*

Aziz Alaoui [d]

[d] *Département de Mathématiques, Université du Havre, BP 540, F-76058 Le Havre Cedex, France*

Abstract

When a set of non linear differential equations is investigated, most of time there is no analytical solution and only numerical integration techniques can provide accurate numercial solutions. In a general way the process of numerical integration is the replacement of a set of differential equations with a continuous dependence on the time by a model for which these time variable is discrete. When only a numerical solution is researched, a fourth-order Runge-Kutta integration scheme is usually sufficient. Nevertheless, sometimes a set of differential equations may be required and, in this case, standard schemes like the forward Euler, backward Euler or central difference schemes are used. The major problem encountered with these schemes is that they offer numerical solutions equivalent to those of the set of differential equations only for sufficiently small time step. In some cases, it may be of a great interest to possess difference equations with the same type of solutions as for the differential equations when the time step is sufficiently large. Non standard schemes as introduced by Mickens [1] allow to obtain more robust difference equations. In this paper, using such non standard scheme, we propose some difference equations as discrete analogues of the Rössler system for which it is shown that the dynamics

is less dependent on the time step size than when a non standard scheme is used. In particular, it has been observed that the solutions to the discrete models are topologically equivalent to the solutions to the Rössler system as long as the time step is less than the threshold value associated with the Nyquist criterion.

Key words: Non linear dynamical systems, discretization, numerical instabilities, global modeling
PACS: 05.45.+b

---

1 Introduction

Until recently, most of the physical processes have been modeled by differential equations where the processes are assumed to be evolving continuously. When these differential equations are non linear, there is very often no analytical solution and only numerical integration techniques can provide accurate numerical solutions to the original differential equations. With the advent of digital computers, this is easily done using a fourth-order Runge-Kutta integration scheme. Nevertheless, sometimes it is necessary to replace the set of differential equations with a continuous dependence on time by a set of difference equations with a discrete time variable. When standard schemes as the forward Euler, backward Euler or central difference schemes is used, the discrete system has solutions which are equivalent to those of the continuous counterpart only for sufficiently small discretization time step. With standard scheme, the upper value of the time step for which the solutions are equivalent to the continuous counterpart is significantly smaller than the sampling time used for recording the time evolution of a physical quantity. The question of a possible equivalence between differential equations for quite large time step has thus emerged as well as a new scientific theory advocating the discreteness of time has emerged [2,3].

This equivalence is particularly important to address when a comparison between different global modeling techniques is attempted. Typically, a global modeling technique is used for obtaining a set of equations that captures the dynamics described by a recorded time series. Such a technique is based on the following procedure. First, a phase space is reconstructed from the measured time series using either delay or derivatives coordinates [4]. If derivative coordinates are used then we obtain a system of ordinary differential equations whose dimensions are equal to the dimensions of the original phase space [5]. On the other hand, if delay coordinates are used then a set of difference equations is obtained. Most of time, the dimensions of the obtained models are significantly greater than those of the original systems [6,7]. Such a feature was never considered as a major problem since Takens proposed an

* Corresponding author. Email address : Christophe.Letellier@coria.fr

existence theorem which ensures the existence of a reconstructed phase space that is diffeomorphically equivalent to the original phase space as long as the dimension of the former is sufficiently large [8]. Indeed, Takens' criterion corresponds to a dimension significantly greater than the dimension of the original phase space. Tempkin and Yorke [9] showed that for almost any choice of measurements (in the sense of prevalence), there exists a scalar difference equation that describes the evolution of the sequence of measurements whose dimension is larger than twice the box-counting dimension of the dynamical system's attractor.

Nevertheless, according to recent works [10–12] where both types of techniques were applied successfully to the same data sets, the dimensions and the number of terms of the obtained global models are different and very much dependent on the techniques used. No direct comparison between the difference and the differential models was therefore possible. Moreover, the obtained global discrete model strongly depends on the discretization time-step size [13]. Consequently, it becomes an important task to compare the global models provided by these modeling techniques. It then appears obvious that, before being able to address correctly this problem, it is necessary to have a clear idea of the possible equivalence between differential equations with time step comparable to the sampling time.

For all the above-mentioned reasons, we decided to reinvestigate the possible equivalence between difference and differential equations. This is obviously connected to the important problem of finding a discretization of a set of ordinary differential equations [1,14,15]. In this context, it is well known that the discretization of continuous equations may have solutions which depend on the discretization time-step size h and numerical instabilities may be encountered. Numerical instabilities are solutions to the discrete finite difference equations that do not correspond to any solution to the original differential equations. Such a feature occurs mainly when the step-size h is too large [16]. This may also be encountered when the order of the difference equations is larger than that of the differential equations [1].

A simple example of numerical instabilities is observed in the discretization of the logistic map using the Euler scheme. Indeed, the elementary nonlinear ordinary differential equation

$$\dot{x}(t) = x(t)\,[1 - x(t)] \tag{1}$$

has two fixed points $x_1^* = 0$ and $x_2^* = 1$. The first fixed point is unstable while the second is stable. Thus, every solution of $x(t)$ with $x(0) > 0$ is asymptotically stable. Using the Euler-type discretization scheme

$$\frac{x_{n+1} - x_n}{h} \approx \dot{x}_n, \tag{2}$$

where $h > 0$ denotes the discretization step size and x_n the value of $x(t)$ for $t = nh$.

The elementary equation (1) thus becomes

$$x_{n+1} = hx_n \left(1 + \frac{1}{h} - x_n\right), \tag{3}$$

which is a slightly modified logistic map. This difference equation has two fixed points which are still $x_1^* = 0$ and $x_2^* = 1$. Nevertheless, the fixed point x_2^* is stable only for $0 < h < 2$. When the discretization step size h is increased, a period-doubling cascade is observed as well as various chaotic attractors and periodic solutions usually encountered in the logistic map. Consequently, it appears that the discretization of equation (1) is only valid, from the asymptotic behavior point of view, for a finite interval of the discretization step size. In fact, equation (3) may be rewritten as

$$x_{n+1} = \delta_x x_n + \delta_{x^2} x_n^2, \tag{4}$$

where $\delta_x = h+1$ and $\delta_{x^2} = -h$. If we take $\delta_x = \lambda$ and $\delta_{x^2} = -\lambda$, we obtain the usual logistic map, where λ is the bifurcation parameter. It appears that the discretization of equation (1) leads to a discrete equation which has the same structure as the logistic equation since h and λ are closely related. The discretization time step h may be viewed as the bifurcation parameter of the equation. This will be also observed in the less trivial case of the Rössler system as discussed in this paper.

Indeed, we will take advantage of the chaotic Rössler system when investigating, in a more precise way, the possible equivalence between a set of ordinary differential equations and its discretization. The case of the Rössler system, which is a simple set of three ordinary differential equations generating a chaotic behavior, will be used because the behavior of such a system allows us to use topological analysis [17] providing a quite accurate characterization of the asymptotic behavior. In a rigorous way, difference and differential equations are said to have the same general solution if and only if $u_n = u(t_n) \mid_{t=nh}$ for $h > 0$. Here, we will investigate a weaker equivalence in terms of solutions characterized by the same topology in the phase space. Such a topological equivalence will be very helpful to distinguish displacement in the parameter space from numerical instabilities. Indeed, we will observe that when the discretization time stepsize is varied, the solution to the discretization model corresponds to a solution of the continuous counterpart with a displacement in the parameter space.

The rest of the paper is organized as follows. Section 2 briefly describes the topology of two characteristic solutions of the Rössler system. In Section 3, different non standard discretization schemes are used and their solutions are investigated versus the discretization time step. A discretization of the analytical model, which is obtained when a single variable is "measured," is proposed and some comments on how it relates to the estimation of models from time series are given. Our conclusions are given in Section 4.

2 Rössler system

Let us start by briefly describing two typical solutions to the Rössler system [18] reading as:

$$\begin{cases} \dot{x} = -y - z \\ \dot{y} = x + ay \\ \dot{z} = b + xz - cz \end{cases} \tag{5}$$

where (a, b, c) are the bifurcation parameters. The Rössler system has two fixed points given by

$$\begin{cases} x_{\pm} = \dfrac{c \pm \sqrt{c^2 - 4ab}}{2} \\ y_{\pm} = -\dfrac{c \pm \sqrt{c^2 - 4ab}}{2a} \\ z_{\pm} = \dfrac{c \pm \sqrt{c^2 - 4ab}}{2a} \end{cases} \tag{6}$$

For $a = 0.432$, $b = 2$ and $c = 4$, the Rössler system has a chaotic attractor for solution (Fig. 1a). According to Farmer *et al* [19], we designate this attractor as the *spiral* attractor. This attractor is characterized by a first-return map to the Poincaré section

$$P \equiv \left\{ (y_n, z_n) \in \mathbb{R}^2 \mid x_n = x_-, \dot{x}_n > 0 \right\}, \tag{7}$$

which is unimodal (Fig. 1b). Thus, the map is constituted by an increasing monotonic branch and a decreasing branch separated by the critical point located at the maximum (Fig. 1b). The critical point defines the generating partition of the attractor which allows encoding of all periodic orbits embedded within the attractor [20]. The increasing branch is very close to the bisecting line and, consequently, the symbolic dynamics is almost complete. A two-symbol symbolic dynamics is complete when all periodic orbits which can be encoded with these two symbols are solutions to the Rössler system. Thus, for $a = 0.432$, most of periodic orbits encoded with two symbols are embedded within the attractor generated by the Rössler system.

When the bifurcation parameter a is increased, new periodic orbits are created and the chaotic attractor increases in size (Fig. 2b). The corresponding first-return map is constituted by more than two branches and, for $a = 0.556$, up to eleven monotonous branches may been identified [20]. The corresponding attractor is designated as the

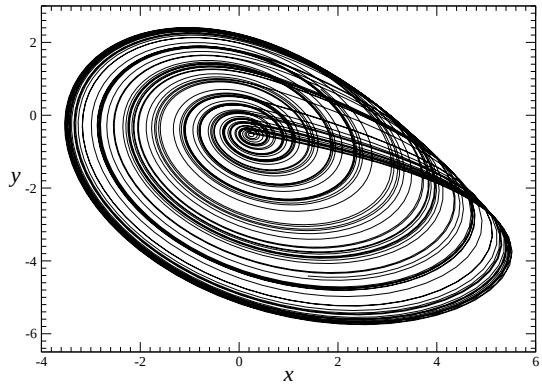

(a) Phase portrait

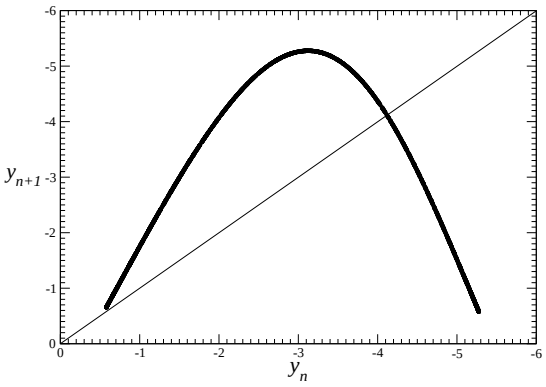

(b) First-return map to the Poincaré section P

Fig. 1. Spiral attractor generated by the Rössler system (5) with the bifurcation parameters $(a, b, c) = (0.432, 2, 4)$.

funnel attractor [19]. For a greater than 0.556, there is metastable chaos, that is the trajectory visits the neighborhood of the unstable periodic orbits solution to the Rössler attractor before being ejected to infinity [20]. The dynamics of the Rössler system can therefore be investigated for $a < 0.556$, b and c remaining constant.

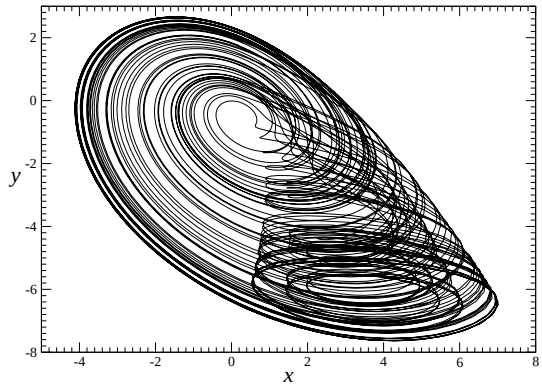

(a) Phase portrait

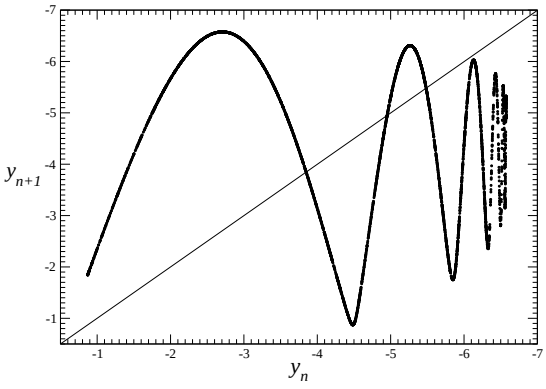

(b) First-return map to the Poincaré section P

Fig. 2. Funnel attractor generated by the Rössler system (5) with the bifurcation parameters $(a, b, c) = (0.556, 2, 4)$.

A bifurcation diagram synthesizes the evolution of the dynamics under the change of the bifurcation parameter a (Fig. 3). The bifurcation parameter a is varied over the interval $[0.432, 0.556]$. We will show that quite similar dependences of the dynamics on the bifurcation parameter is recovered when the discretization time step h of the discretization of the Rössler system is increased.

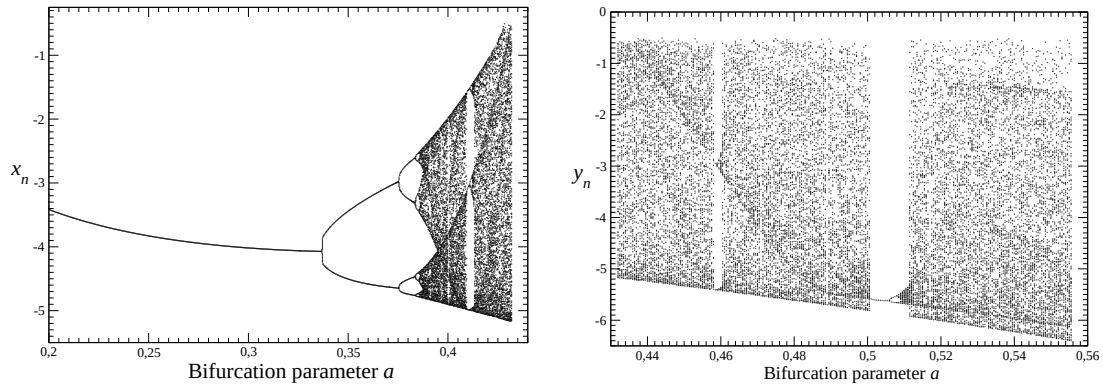

(a) $a < 0.432$ (b) $a > 0.432$

Fig. 3. Bifurcation diagram versus the bifurcation parameter a of the Rössler system (5). Part (a) corresponds to values smaller than 0.432 here used as a reference and (b) for values larger than this reference.

3 Analytical discretization of continuous systems

3.1 Mickens' guidelines

It is known that discretization of nonlinear differential equations $\dot{\boldsymbol{u}}_i = \boldsymbol{f}_i(\boldsymbol{u}_j)$ may have chaotic behavior while its differential counterpart has a limit cycle or, even just a stable fixed point. Lorenz showed that the discretization version of a simple set of two nonlinear differential equations may exhibit chaotic solutions for sufficiently large values of the discretization time step [21] and Whitehead & McDonald showed that the discretization of a two-dimensional nonlinear system can exhibit a chaotic regime [22]. In order to improve the discretization scheme, Mickens formulated a basic set of rules for constructing nonstandard schemes for differential equations [23]. We start from the general form

$$\dot{u} \mapsto \frac{u_{k+1} - \Psi u_k}{\varphi}, \tag{8}$$

where Ψ and φ depends on the step-size h and other parameters occurring in the differential equations. Functions Ψ and φ should satisfy the conditions

$$\begin{cases} \Psi = 1 + O(h) \\ \varphi = h + O(h^2) \end{cases} \tag{9}$$

and may vary from one equation to another. Unfortunately, there is no clear prior set of guidelines for determining them. In most applications, Ψ is usually selected to be $\Psi = 1$, and φ is determined by the requirement of having the correct stability

properties for special solutions to the differential equations. A general choice for φ may be

$$\varphi_i(h, g_i) = \frac{1 - e^{-g_i h}}{g_i}, \tag{10}$$

where g_i's are determined as follows. Let $\boldsymbol{u}_j$ denote the coordinates of the j^{th} fixed point of the continuous system to discretize. The function g_i is then equal to

$$g_i = \max \left(\left| \frac{\partial f_i}{\partial u_i} \right|_{\boldsymbol{u}=\boldsymbol{u}_j} \right). \tag{11}$$

The search over all fixed points allows to identify the fastest time scale and to "normalize" the time according to it. The functions φ_i can be interpreted as a "normalized" or a rescaled time-step size such that its value is never larger than the smallest time scale of the system. Since many of the mechanisms that lead to the occurrence of numerical instabilities have their origin in using a step-size that is greater than some relevant physical time scale, this method for selecting φ_i's reduces these types of instabilities. In other words, the use of functions φ_i, rather than just h, allows the value of h to be much larger than the one normally selected because it is the effective step-size φ_i that determines the stability and not the actual step-size h. Another issue of great importance is that, in general, nonlinear terms are modeled by discrete expressions that are non local on the computational grid [23]. For instance, a u^2 term would be replaced by $u_{k+1}u_k$ in the finite difference scheme, whereas conventional methods would use the local form u_k^2. An important rule to build discretization is that the discrete equations should be equal to the order of the corresponding derivatives of the differential equations, otherwise spurious solutions (numerical instabilities) will occur [1]. The fundamental reason for the existence of numerical instabilities is that the discrete models of differential equations have a larger parameter space than the corresponding differential equations. This is easily argued by the fact that the time-step size h can be regarded as an additional parameter. Even if $\{y(,\lambda)\}$ and $\{y_k(\lambda, h)\}$ are "close" to each other for a particular value of h, say $h = h_1$, if h is changed to a new value, say $h = h_2$, the possibility exists that $y_k(\lambda, h_2)$ differs greatly from $y_k(\lambda, h_1)$ both qualitatively and quantitatively [1].

Our aim is to show how this type of discretization scheme may influence the quality of the model and its sensitivity to the choice of the discretization time-step size h. We will investigate three different discretizations. The last one follows all of Mickens' recommendations.

3.2 One simple example

The first discrete model is obtained using the following transformation on system (5)

$$\left|\begin{array}{l} x \mapsto x_k \\ y \mapsto y_k \\ z \mapsto z_k \\ xz \mapsto x_k z_{k+1}. \end{array}\right. \tag{12}$$

Thus, by applying the discretization scheme (8) with $\Psi = 1$, we obtain the model:

$$\left\{\begin{array}{l} x_{k+1} = x_k - \varphi_1(y_k + z_k) \\ \\ y_{k+1} = (1 + a\varphi_2)y_k + \varphi_2 x_k \\ \\ z_{k+1} = \dfrac{z_k(1 - c\varphi_3) + b\varphi_3}{1 - \varphi_3 x_k}, \end{array}\right. \tag{13}$$

where the functions are chosen according to

$$\varphi_1 = \varphi_2 = \varphi_3 = \sin h \tag{14}$$

Note that introducing the non local term $x_k z_{k+1}$ induces the rational form of the third equation. Depending on the choice of the functions φ_i, the discretization of the Rössler system may be stable over a wider interval of the discretization time step h as discussed below.

For a very small discretization time step h, the dynamics underlying the difference equations (13) with φ defined by relation (14) is topologically equivalent to the dynamics of the Rössler system (5). This means that the phase portrait (Fig. 4a) solution of the difference equations (13) with φ_i's defined by relation (14) is also characterized by a first-return map to a Poincaré section (Fig. 4b) equivalent to the one associated with the Rössler dynamics (Fig. 1b). The populations of periodic orbits embedded within the attractors solution of the Rössler system and its discretization are the same. Moreover, both attractors are characterized by the same template, that is, periodic orbits have the same relative organization in the phase space. In other words, the relative organization of periodic orbits may be described by the same branched manifold.

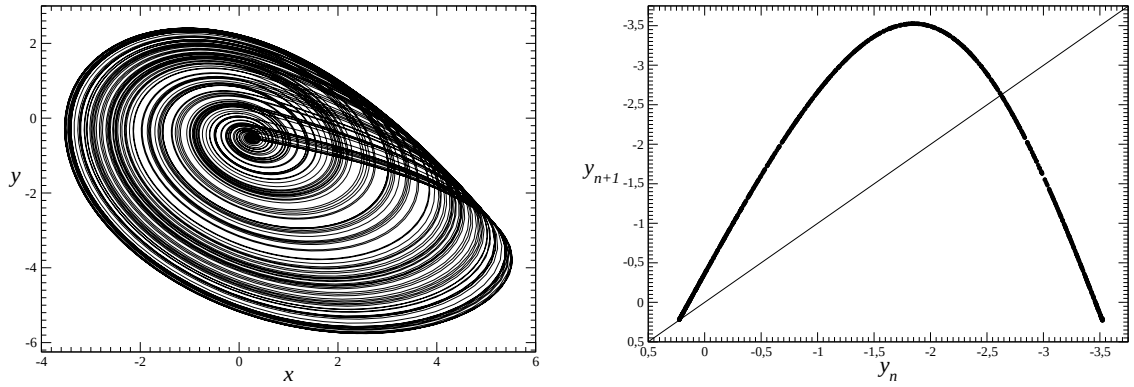

(a) Spiral attractor (b) First-return map

Fig. 4. Spiral chaotic attractor solution of the difference model (13) for the time step $h = 0.001$ s with the functions φ_i given in relation (14).

Nevertheless, when the discretization time step h is increased, bifurcations occur and new periodic orbits are created or destroyed. For larger values of h, the first-return map presents new monotonous branches (Fig. 5b) as observed on the Rössler attractor of the funnel type (Fig. 2b). This means that the discretization time step h may be considered as a bifurcation parameter, which plays the same role as the parameter a does for the Rössler system. Indeed, when h is varied over the range $(0.0, 0.0924)$, the bifurcation diagram (Fig. 6) is rather similar to the one computed versus the a parameter for the Rössler system (Fig. 3b). This discretization of the Rössler system has a chaotic attractor for solution that is topologically equivalent to one solution to its continuous counterpart but with different bifurcation parameter values as long as the discretization time step is sufficiently small. Consequently, the discretized version of the Rössler system remains valid for quite large values of the time step h. Varying the value of the time step h, therefore, corresponds to a displacement in the parameter space.

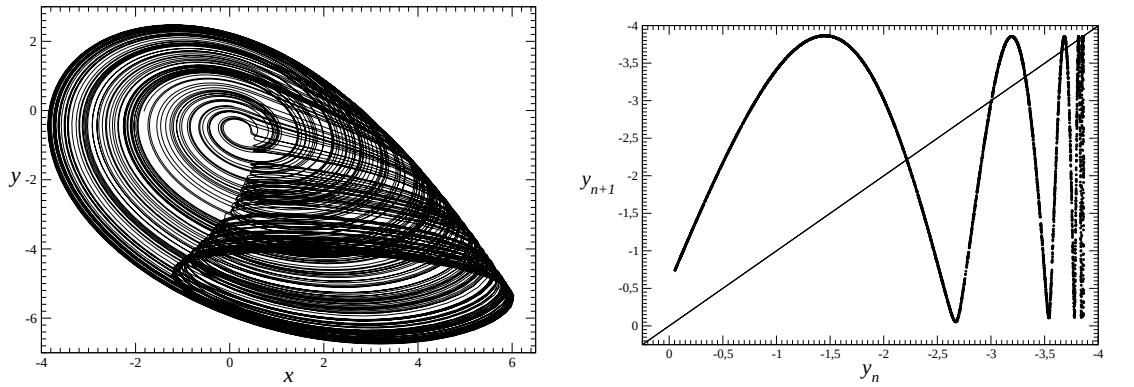

(a) Funnel attractor (b) First-return map

Fig. 5. Funnel chaotic attractor solution of the difference model (13) for the time step $h = 0.0924$ s with the functions φ_i given in relation (14).

Note that the time step cannot be varied over a very large range. In fact, the interval is restricted to a limited range because for values beyond 0.0924 s, the trajectory is ejected to infinity as was observed when the a parameter is varied.

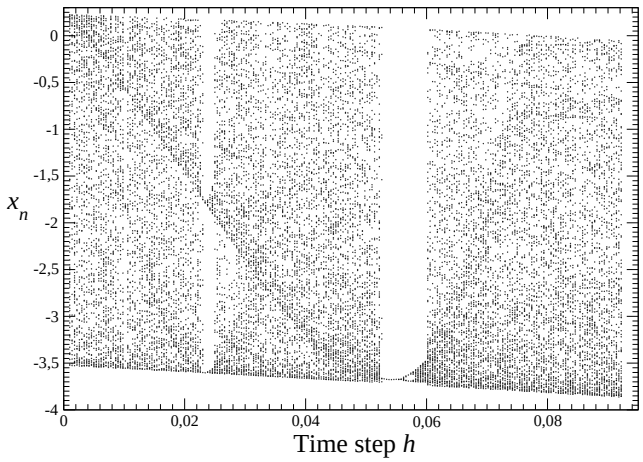

Fig. 6. Bifurcation diagram versus the time step h for model (13) with the functions φ_i given in relation (14). Compare with Fig. 3.

Such a modification of the dynamics through the discretization procedure is a common feature observed in global modeling. Indeed, very often the global model estimated from experimental time series does not exhibit exactly the same behavior than the experimental one. This does not mean that the model is bad since, very often, a parameter of the model may be slightly varied to recover the expected dynamics [24]. In other words, for a given value of the time step h, it is possible to modify the bifurcation parameters in order to recover the expected dynamics. For instance, with $h = 0.0924$ s, a two branch first-return map is recovered with $a = 0.321$. In that case, the development of the dynamics induced by the increase of the discretization time step h is canceled out by the decrease of the a parameter. This feature results directly from the coefficient $(1 + a\varphi_2)$ in the second equation (13) since it is the coefficient of the autoregressive part of the equation. The term $(1 + a\varphi_2)$ therefore defines the overall dynamics, the second term $\varphi_2 x_k$ being only the forcing function (the exogenous part of the equation). Since $\varphi_2 = \sin h$, the increase of h has to be followed by the decrease of a in order to keep the coefficient $(1 + a\varphi_2)$, and therefore the dynamics of the second equation of (13) constant. Of course, the dynamics of the whole system (13) depends on other things but the compensating effect of a over h is partially explained by this remark.

3.3 An optimized finite difference model

In disrete model (13), we used the non local nonlinear term $x_k z_{k+1}$. It is also possible to choose the other form ${}_{k+1}z_k$. In this case, the third equations becomes polynomial

$$z_{k+1} = b\varphi_3 + [1 + \varphi_3 (x_{k+1} - c)] z_k \tag{15}$$

and the time step can be increased up to 0.2405 s which is 2.5 times greater than the upper value reached with discretized model (13). The bifurcation diagram thus obtained is very similar as the bifurcation diagram shown in Fig. 6, but with a rescaling of the a-axis between 0 and 0.2405 s.

A more robust discrete model is obtained when we follow all the recommendation given by Mickens for constructing new finite difference equations corresponding to the Rössler system. We use the following transformation

- first equation: $(x_k, y_k, z_k) \mapsto (x_k, y_k, z_k)$
- second equation: $(x_k, y_k, z_k) \mapsto (x_{k+1}, y_k, z_k)$
- third equation: $(x_k, y_k, z_k) \mapsto (x_{k+1}, y_{k+1}, z_k)$.

and the nonlinearity xz replaced by the non local term $x_{k+1}z_k$. This choice has also the advantage of preserving a polynomial form for the discretization model. Function Ψ is equal to 1. Thus, we obtain

$$\begin{cases} x_{k+1} = x_k - \varphi_1(y_k + z_k) \\ y_{k+1} = (1 + a\varphi_2)y_k + \varphi_2 x_{k+1} \\ z_{k+1} = b\varphi_3 + [1 + \varphi_3 (x_{k+1} - c)] z_k \end{cases} \tag{16}$$

The function φ_i is chosen according to the on-diagonal elements of the Jacobian matrix of the original continous system (5)

$$J_{ij} = \begin{bmatrix} 0 & -1 & -1 \\ 1 & a & 0 \\ z & 0 & x - c \end{bmatrix} \tag{17}$$

Note that since $J_{11} = 0$, there is no natural time scale associated with the autoregressive part of the first equation. We therefore choose choose the function φ_1 equal to h, thus expressing this lack. According to equations (10) and (11), the second function is

$$\varphi_2 = \frac{1 - e^{-ah}}{a} \tag{18}$$

and the third one is

$$\varphi_3 = \frac{1 - e^{-x_c h}}{x_c} \tag{19}$$

where $x_c = \frac{-c+\sqrt{c^2-4ab}}{2}$ is estimated using the fixed point coordinates and equation (11). Note that the optimized model (16) is polynomial.

This discrete model can be iterated with a discretization time-step size h over the range $(0, 0.6194)$, that is over an interval three time larger than with the previous discretization schemes. The bifurcation diagram versus h (Fig. 7) is very similar to the diagrams computed with the continuous Rössler system versus the a parameter (Fig. 3). But note that increasing h is similar to a decrease of parameter a. This may be understood by replacing x_{k+1} in second equation of system (16) by the first equation of this system : we thus obtain

$$y_{k+1} = [1 + \varphi_2(a - \varphi_1)]\, y_k + \varphi_2 x_k - \varphi_1 \varphi_2 z_k \tag{20}$$

where in the term $[1 + \varphi_2(a - \varphi_1)]\, y_k$, $\varphi_1 = h$ tends to balance the effect of parameter a. The bifurcation diagram (Fig. 7) thus means that all behavior solutions to the discretization of the Rössler system are topologically equivalent to the solution to the continuous counterpart for appropriate values of the bifurcation parameters. Note that when $h \in]0, 0.05]$, very few bifurcations are observed and, consequently, the dependence to the solution of the discrete model (16) on the time step-size h is very weak. This model is therefore very robust against increase of the time step h.

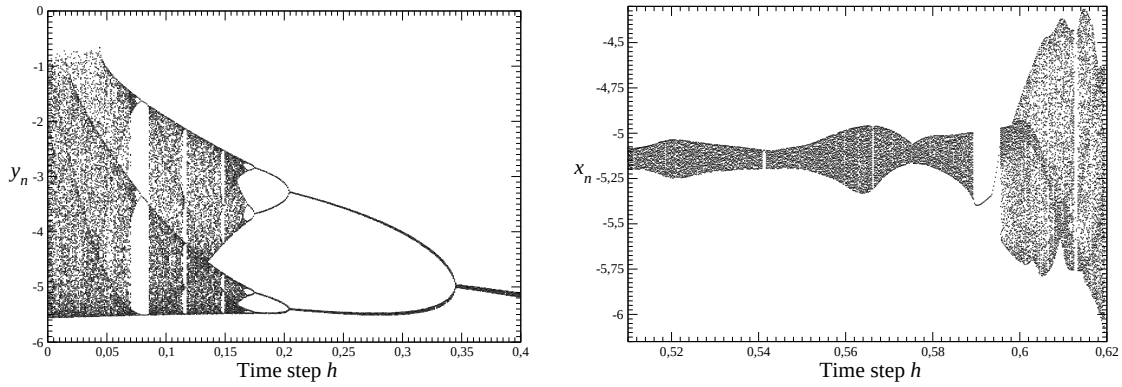

(a) Under the Nyquist's criterion (b) Beyond the Nyquist's criterion

Fig. 7. Bifurcation diagram versus the time step h for the optimized discrete model (16) with the functions φ_i given in relations (18) and (19). Numerical instabilities occur when the discretization time step is greater than the Nyquist's criterion (b).

The pseudo-period of the original Rössler system is 6.3 s as given by the main frequency $f_0 = 0.1587$ Hz (Fig. 8). The largest significant frequency which may be identified on the power spectrum is $f_{\max} \approx 1$ Hz. According to the Nyquist's criterion, the sampling frequency should be greater than $2f_{\max}$, that is around 2 Hz. This means that it would not be possible to get a sufficient amount of information to describe the dynamics if the sampling rate were lower. Such a threshold corresponds to a sampling time $\Delta t \approx 0.5$ s. It is interesting to note that the behaviors, which are no longer topologically equivalent to the solution to the original Rössler system,

appears for discretization time-step size h greater than the critical sampling time corresponding to the Nyquist's criterion.

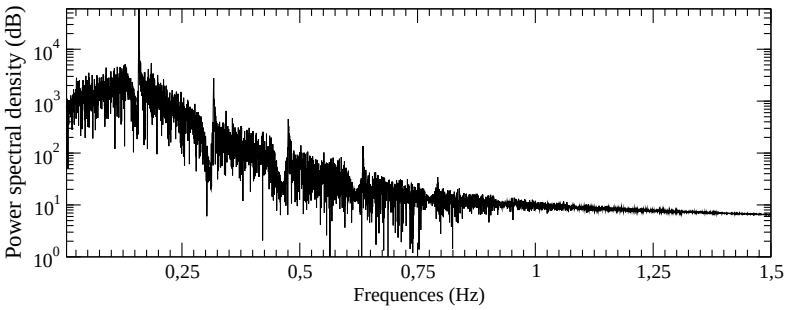

Fig. 8. Fourier spectrum of the Rössler system with $(a, b, c) = (0.432, 2, 4)$. The main frequency f_0 is equal to 0.1587 Hz which corresponds to a pseudo-period equal to 6.3 s. The highest significative frequency $f_{\max} \approx 1.9$ Hz.

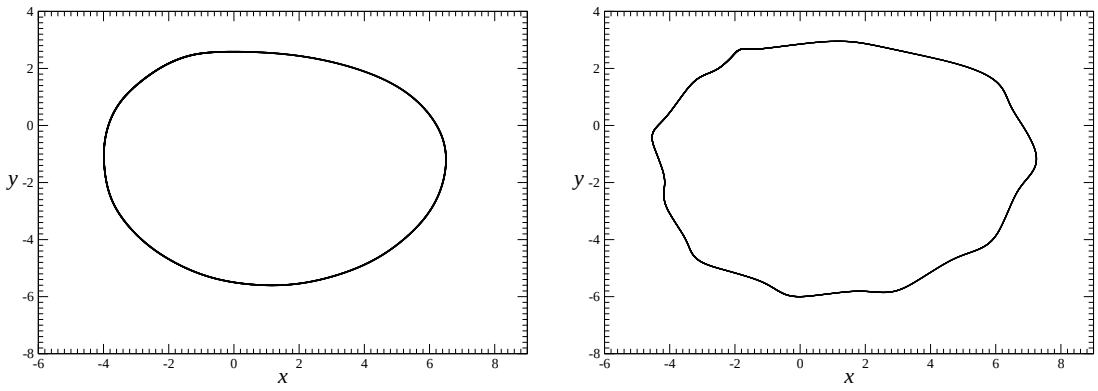

(a) $h = 0.500$ s (b) $h = 0.580$ s

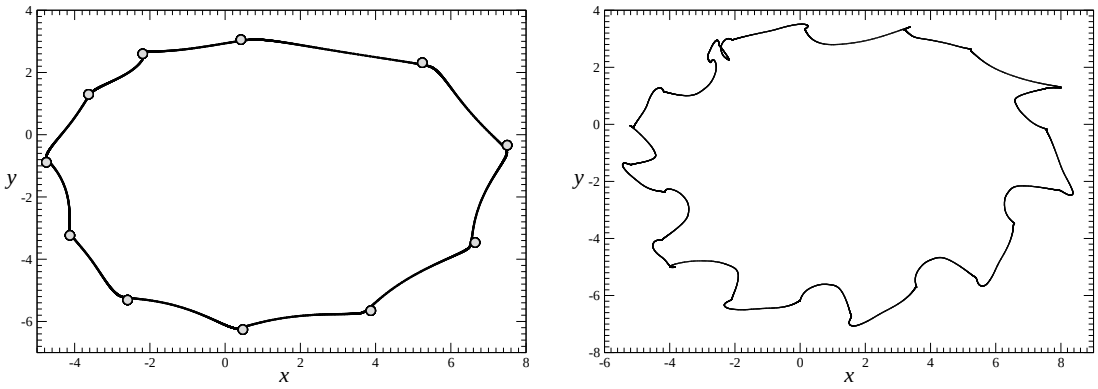

(c) $h = 0.589$ s (d) $h = 0.6194$ s

Fig. 9. Solutions to the optimized discrete model of the Rössler system for different values of h.

Indeed, for $h = 0.5$ s, a period-1 limit cycle (Fig. 9a), which is still obviously topologically equivalent to the period-1 limit cycle of the original Rössler system, is observed if the limit cycle is progressively constrained by the heterocline connections between the periodic points of an unstable period-11 orbit (Figs. 9b and 9c).

With $h = 0.589$ s, the limit cycle is shown with the unstable periodic orbit (Fig. 9c) on the continuous Rössler system and, consequently, results from numerical instabilities. When the time step is increased, the limit cycle presents apparent cusps which are actually points of extreme curvature. A similar phenomena has been observed by Lorenz [21]. Unfortunately, the discrete model is not sufficiently stable to remain stable for a higher discretization time step but we may expect that spurious chaotic behavior would have been observed in such a case. This was observed by Lorenz [21] and in another investigation using another scheme for discretizing another system [25,26].

Note that numerical instabilities appear when the discretization time step h is greater than the Nyquist's criterion. Indeed, the Nyquist criterion is a criterion for the sampling rate of a continuous variable which guarantees that there is no spectra superposition. In other words, this criterion provides an upper value for the time-step zise at which the time series must be sampled. With greater time stepsize, some information is lost and the dynamics cannot be fully recovered from the measurements. By analogy, we conjecture that when a discretization of a continuous system is built and iterated with a discretization time stepsize h greater than the Nyquist criterion, the dynamics cannot be longer recovered without any damage. Consequently, the solutions thus observed are expected to not correspond to a solution to the original differential system, even with a displacement in the parameter space. This is directly related to a comment made by Mickens [23] who stated that numerical instabilities can occur when the finite difference equations do not satisfy a condition that is of importance for the corresponding differential equations. The main time scale of the dynamics is definitely an important characteristic and choosing the time step without any consideration related to this property does not make sense. This means that we obtained difference equations which have the best equivalence with the Rössler dynamics, that is, which have solution topologically equivalent to some solution to the Rössler system with a possible displacement in the parameter space.

4 Differential embedding versus delay embedding

When one is facing a real system, he usually has a single time series $\{s(t)\}$ for investigating the dynamics and the first step is to reconstruct the phase space. Two main choices are: using the delay coordinates $\{s(t), s(t+\tau), s(t+2\tau), ...\}$ or using the derivative coordinates $\{s(t), \dot{s}(t), \ddot{s}(t), ...\}$. In the first case, a discrete-time model will be attempted [6] while in the second, a continuous-time model has to be estimated [5]. Thus difference or differential equations may be estimated depending on the kind of the embedding chosen. Recent works [10–12] suggest that both approaches are more or less equivalent although rigorous results are still lacking. As already discussed, the main point preventing us from careful investigations about such equivalence was that the structure selection technique implemented for select-

ing the relevant terms and the dimensionality of the difference equations estimated from the time series [27] usually provides difference equations with a dimensionality greater than the one obtained with differential equations although, in general, with far less terms than the continuous counterpart has. Increasing the dimensionality of the difference equations helps to obtain models more stable and simpler from an algebraic point of view, that is, in the number of terms involved and in the order of nonlinearities. Note that the dimensionality of the differential model buil on derivative coordinates cannot be varied. It is strongly constrained by the smallest dimension with which the phase portrait may be represented without self-intersections, that is by the so-called embedding dimension [28,29]. Therefore, it becomes obvious that it is quite difficult to establish a link between equations working in spaces with different dimension.

In order to show that an equivalence between a discrete model and a differential one is possible to establish, we will compute a discretization of the differential model induced by the y-variable of the Rössler system. Since the equations of the system are known, it is possible to analytically derive such a differential model. Let us assume that the y-variable of the Rössler system is measured. In such a case, the phase space may be reconstructed using the derivative coordinates

$$\begin{cases} X = y \\ Y = \dot{y} \\ Z = \ddot{y} \end{cases} \tag{21}$$

The reconstructed space has a dimension equal to 3, in agreement with the embedding dimension which can be computed using the false nearest neighbors technique [29]. The derivatives may be expressed analytically using the Lie derivatives defined as

$$L_f\Phi(\boldsymbol{x}) = \sum_{k=1}^{3} f_k(\boldsymbol{x}) \frac{\partial \Phi(\boldsymbol{x})}{\partial \boldsymbol{x}_k} \tag{22}$$

and recursively for the higher-order derivatives $L_f^j\Phi(\boldsymbol{x}) = L_f\left(L_f^{j-1}\Phi(\boldsymbol{x})\right)$. Here the Rössler system $\dot{\boldsymbol{x}} = \boldsymbol{f}(\boldsymbol{x})$ is observed using $s = \Phi(\boldsymbol{x}) = y$. The function $\Phi : \mathbb{R}^3(x,y,z) \to \mathbb{R}(y)$ is here a smooth function called the *measurement function*. Thus, the derivatives are equal to

$$\Theta \equiv \left| \begin{array}{lll} X = \Phi(\boldsymbol{x}) & & = y \\ Y = L_f\Phi(\boldsymbol{x}) = f_2(\boldsymbol{x}) & & = x + ay \\ Z = L_f^2\Phi(\boldsymbol{x}) = f_1(\boldsymbol{x})\frac{\partial f_2}{\partial x} + f_2(\boldsymbol{x})\frac{\partial f_2}{\partial y} + f_3(\boldsymbol{x})\frac{\partial f_2}{\partial z} & & = ax + (a^2-1)y - z. \end{array} \right. \tag{23}$$

Note that this coordinate transformation $\Theta : \mathbb{R}^3(x,y,z) \rightarrow \mathbb{R}^3(X,Y,Z)$ defines a diffeomorphism between the original phase space $\mathbb{R}^3(x,y,z)$ and the differential space $\mathbb{R}^3(X,Y,Z)$ spanned by the successive derivatives of y.

A general form for the differential model induced by the y-variable of the Rössler system reads as:

$$\begin{cases} \dot{X} = Y \\ \dot{Y} = Z \\ \dot{Z} = F(X,Y,Z) = L_f^3 \, \Phi(\boldsymbol{x}) \end{cases} \tag{24}$$

where $F(X,Y,Z)$ is the model function which has to be estimated [5]. In our case, since we know the equations of the original system, this function can be computed analytically. To express the function $F(X,Y,Z)$ in terms of derivative coordinates, the coordinate transformation $\Theta : \mathbb{R}^3(x,y,z) \rightarrow \mathbb{R}^3(X,Y,Z)$ given by relation (23) has to be inverted:

$$\Theta^{-1} \equiv \left| \begin{array}{l} x = -aX + Y \\ y = X \\ z = -X + aY - Z \end{array} \right. \tag{25}$$

Thus, the model function reads as [30]:

$$\begin{aligned} F(X,Y,Z) = & -b - cX + (ac-1)Y + (a-c)Z - aX^2 \\ & +(a^2+1)XY - aXZ - aY^2 + YZ. \end{aligned} \tag{26}$$

Such a three-dimensional differential model may be discretized as done for the Rössler system in the previous section. Using the scheme (12), we obtain

$$\begin{cases} X_{k+1} = X_k + \varphi_1 Y_k \\ Y_{k+1} = Y_k + \varphi_2 Z_k \\ Z_{k+1} = \dfrac{\left[-b - cX_k + (ac-1)Y_k + (a-c)Z_k - aX_k^2 + (a^2+1)X_kY_k - aY_k^2\right]\varphi_3 + Z_k}{1 + \varphi_3(aX_k - Y_k)} \end{cases} \tag{27}$$

with $\varphi_1 = \varphi_2 = \varphi_3 = \sin h$. An integration of this discretization generates an attractor (Fig. 10a) topologically equivalent to the Rössler system for $h = 0.001$ s. As observed for the various discretizations of the Rössler system, when the discretization

time step h is increased, the attractor, which is of the spiral type for small values of h (Fig. 10a), becomes progressively a funnel type attractor (Fig. 10b).

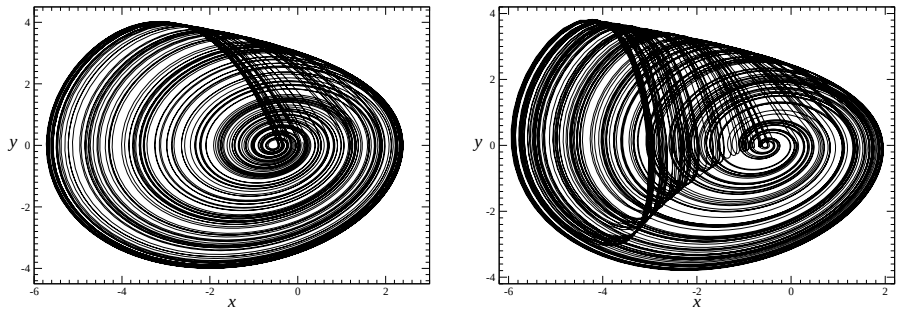

(a) $h = 0.001$ s (b) $h = 0.101$ s

Fig. 10. Discretization of the differential model (27) by the y-variable using Mickens' scheme.

When the discretization time step h is varied, a bifurcation diagram is obtained (Fig. 11a). It is very similar to the diagram of the Rössler system for $a > 0.432$ (Fig. 7b). As we observed for the Rössler system, it is possible to vary the bifurcation parameter to increase the interval over which the discretization time step may be varied. For instance, with $h = 0.101$ s, the a-bifurcation parameter has to be decreased to $a = 0.338$ to recover the spiral attractor with its unimodal map. For this value of a, the discretization time step may be increased up to $h = 0.162$ s (Fig. 11b to compare with Fig. 7a and 7b) and with $a = 0.200$, h may be increased up to 0.253 s. As observed for the discretization of the Rössler system, the difference equation describing the phase portrait reconstructed using delay coordinates have solution attractors which are topologically equivalent to attractors solution to the Rössler system. Moreover, when the bifurcation parameters are varied, the spiral attractor may be recovered for any value of the discretization time step less than 0.253 s. Note that such a time step h corresponds to roughly 1/25 of the pseudo-period equal to 6.2 s. This is still a very small value since difference equations have been estimated numerically using the technique described in [27] with a time step around to 1.0 s!

We tried to apply Mickens' recommendations as done in the previous section. The obtained discrete model reads as:

$$\begin{cases} X_{k+1} = X_k + \varphi_1 Y_k \\ Y_{k+1} = Y_k + \varphi_2 Z_k \\ Z_{k+1} = [1 + \varphi_3(Y_{k+1} - aX_{k+1} + a - c)]\, Z_k \\ \qquad\qquad + \varphi_3 \left[-b - cX_{k+1} + (ac-1)Y_{k+1} - aX_k X_{k+1} + (a^2+1)X_{k+1}Y_k - aY_k Y_{k+1}\right], \end{cases} \tag{28}$$

where $\varphi_1 = \varphi_2 = h$ and

$$\varphi_3 = \frac{1 - e^{-X_c h}}{X_c}, \tag{29}$$

with $X_c = \frac{c+\sqrt{c^2-4ab}}{2} + a - c$. Unfortunately, this model is less robust against an increase of the discretization time step-size since the trajectory settles down onto the inner fixed point for $h = 0.0424$ s. Changing the functions φ_i's does not change this upper value for h. It is possible that the very particular form of the differential model (26) induced by the y-variable of the Rössler system and some different rules would be used.

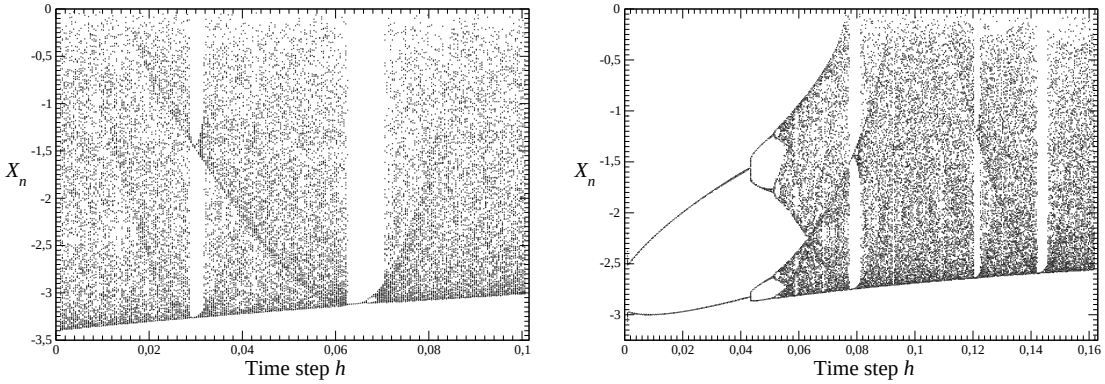

(a) $a = 0.432$ (b) $a = 0.338$

Fig. 11. Bifurcation diagram of the discretization of the differential model induced by the y-variable of the Rössler system for two different values of a.

With this discretization of the differential model induced by the y-variable of the Rössler system, we have an analytical form for the function which is to estimate using NARMA polynomial techniques [6,27]. Thus, it is possible to directly compare the model obtained with these theoretical forms. Note that these discretizations are mainly valid when the discretization time step is small enough and, consequently, can be used for comparison when the sampling rate is high enough. Nevertheless, the form of the first discretization is rational while the NARMA models are polynomials. We thus have a polynomial expansion of such a rational function. For analytical comparison, (28) would be preferred. Since it is possible to obtain the NARMA model with quite a large time step h, the discretization scheme used here cannot be applied anymore and more sophisticated schemes should be used [25]. Also, since a possible form for the NARMA model induced by the y-variable of the Rössler model can be derived, it is now clearer why the NARMA technique provides more or less the same results than a global modeling technique using derivative coordinates [30]. This is reinforced by the theorem proposed by Mickens [1] which states that an exact finite difference scheme of differential equations always exists. Such an exact discrete model is still to be found for the differential model (26).

5 Conclusion

The problem of the possible equivalence between difference and differential equations has been investigated in the case of the Rössler system. Using non standard Mickens' schemes, we showed that the discretizations of the Rössler system have solutions which are topologically equivalent to solutions to the Rössler system with a displacement in the parameter space. This means that varying the time step used in the discretization corresponds to apply a displacement in the parameter space for the original Rössler system. Nevertheless, using a Mickens' non standard discretization scheme, we found a discretization model very robust under discretization time step increases. In this case, it has been observed that as long as the time step is less than the threshold value associated with the Nyquist criterion, the discrete model has solutions which are topologically equivalent to solutions to the original continuous system with appropriate bifurcation parameter values. This is quite important because this means that there exists a possible discrete counterpart to a set of differential equations as long as the time step do not exceed a value related to the Nyquist's criterion. This is all what we need since when a global model is attempted from a time series, the Nyquist's criterion states that the sampling rate has to be lower than this upper value. Of course, the discrete model proposed here has still to be improved. Unfortunately, there is no general guideline for that and other choices for functions φ and Ψ have to be tried. Nevertheless, this study convinced us that a discrete global model of the same dimension as the differential model can be obtained. Such a result already opens new insight for comparing discrete and continuous-time global models.

Acknowledgements

We would like to thank Ronald Mickens for his warm encouragements and helpful remarks to improve this work. C.L. and L.A.A. acknowledge financial support by CNRS and CNPq.

References

[1] R. E. Mickens, *Nonstandard finite difference models of differential equations*, World Scientific, (1994).

[2] K. Inagaki, On the discreteness at the edge of chaos, *IPSJ Trans. Mathematical Modeling and its applications*, **40**, SIG 2(TOM 1), (1999) 76-81.

[3] S. Elaydi, Is the world evolving discretely?, *Advances in Applied Mathematics*, (2003).

[4] N. H. Packard, J. P. Crutchfield, J. D. Farmer & R. S. Shaw, Geometry from a time series, *Physical Review Letters,* **45** (9), (1980) 712-716.

[5] G. Gouesbet & C. Letellier, Global vector field reconstruction by using a multivariate polynomial L_2-approximation on nets, *Physical Review E*, **49** (6), (1994) 4955-4972.

[6] I. J. Leontaritis & S. A. Billings, Input-output parametric models for nonlinear systems part II: Stochastic nonlinear systems, *International Journal of Control*, **41** (2), (1985) 329-344.

[7] R. Brown, N. F. Rul'kov & E. R. Tracy, Modeling and synchronizing chaotic systems from time-series data, *Physical Review E*, **49** (5), (1994) 3784-3800.

[8] F. Takens, Detecting strange attractors in turbulence, *Lecture Notes in Mathematics*, **898**, (1981) 366-381.

[9] J.A. Tempkin & J. Yorke, Measurements of a physical process satisfy a difference equation. *Journal of Difference Equations and Applications*, **8** (1), (2002) 13-24.

[10] C. Letellier, L. A. Aguirre, J. Maquet & A. Aziz-Alaoui, Should all the species of a food chain be counted to investigate the global dynamics?, *Chaos, Solitons & Fractals*, **13**, (2002) 1099-1113.

[11] C. Letellier, L. A. Aguirre, J. Maquet & B. Lefebvre, Analogy between a 10D model for nonlinear wave-wave interaction in a plasma and the 3D Lorenz dynamics, *Physica D*, **179**, (2003) 33-52.

[12] J. Maquet, C. Letellier & L. A. Aguirre, Scalar modeling and analysis of a 3D biochemical reaction model, submitted to *Journal of Theoretical Biology.*

[13] S. A. Billings & L. A. Aguirre, Effects of the sampling time on the dynamics and identification of nonlinear models, *International Journal of Bifurcation & Chaos*, **5** (6), (1995) 1541-1556.

[14] P. Liu & S. N. Elaydi, Discrete competitive and cooperative models of Lotka-Volterra type, *J. Computational Anal. Appl.*, **3**, (2001) 53-73.

[15] H. Al-Kahby, F. Dannan & S. N. Elaydi, Non-Standard discretization methods for some biological models, *Nonstandard finite difference models of differential equations*, Ed. R. E. Mickens, World Scientific, (2000) 155-188.

[16] R. E. Mickens, Genesis of elementary numerical instabilities in finite-difference models of ordinary differential equations, *Proceedings of Dynamic Systems and Applications*, **1**, (1994) 251-258.

[17] R. Gilmore, Topological analysis of chaotic dynamical systems, *Reviews of Modern Physics*, **70** (4), (1998) 1455-1529.

[18] O. E. Rössler, An equation for continuous chaos, *Physics Letters A*, **57** (5), (1976) 397-398.

[19] J. D. Farmer, J. P. Crutchfield, H. Frœling, N. H. Packard & R. S. Shaw, Power spectra and mixing properties of strange attractors, *Annals of the New York Academy of Sciences,* **357**, (1980) 453-472.

[20] C. Letellier, P. Dutertre & B. Maheu, Unstable periodic orbits and templates of the Rössler system: toward a systematic topological characterization, *Chaos*, **5** (1), (1995) 271-282.

[21] E. N. Lorenz, Computational chaos — a prelude to computational instability, *Physica D*, **35**, (1989) 299.

[22] R. R. Whitehead & N. Mc Donald, A chaotic mapping that displays its own homoclinc structure, *Physica D*, **13**, (1984) 401.

[23] R. E. Mickens, Nonstandard finite difference schemes for differential equations, *Journal of Difference Equations and Applications*, **8** (9), (2002) 823-947.

[24] L. A. Aguirre, C. Letellier & J. Maquet, Induced bifurcations in the validation of non linear dynamical models, *International Journal of Bifurcation & Chaos*, **12** (1), (2002) 135-145.

[25] E. M. A. M. Mendes & S. A. Billings, A note on discretization of nonlinear differential equations, *Chaos*, **12** (1), (2002) 66-71.

[26] E. M. A. M. Mendes & C. Letellier, A new discretization scheme for large discretization time step, submitted to *Journal of Physics A*.

[27] L. A. Aguirre & S. A. Billings, Retrieving dynamical invariants from chaotic data using NARMAX models, *International Journal of Bifurcation and Chaos*, **5** (2), (1995) 449-474.

[28] H. D. I. Abarbanel & M. B. Kennel, Local false nearest neighbors and dynamical dimensions from observed chaotic data, *Physical Review E*, **47** (5), (1993) 3057-3068.

[29] L. Cao, Practical method for determing the minimum embedding dimension of a scalar time series, *Physica D*, **110** (1 & 2), (1997) 43-52.

[30] C. Letellier, J. Maquet, L. Le Sceller, G. Gouesbet & L. A. Aguirre, On the non-equivalence of observables in phase space reconstructions from recorded time series, *Journal of Physics A*, **31**, (1998) 7913-7927.